Biophysical Journal
Article

Biophysical Society

Binding Modes of Phthalocyanines to Amyloid β Peptide and Their Effects on Amyloid Fibril Formation

Ariel A. Valiente-Gabioud,[1] Dietmar Riedel,[2] Tiago F. Outeiro,[3,4,5] Mauricio A. Menacho-Márquez,[1] Christian Griesinger,[4,6] and Claudio O. Fernández[1,6,*]

[1]Max Planck Laboratory for Structural Biology, Chemistry and Molecular Biophysics of Rosario (MPLbioR, UNR-MPIbpC) and Instituto de Investigaciones para el Descubrimiento de Fármacos de Rosario (IIDEFAR, UNR-CONICET), Universidad Nacional de Rosario, Ocampo y Esmeralda, Rosario, Argentina; [2]Facility for Transmission Electron Microscopy, Max Planck Institute for Biophysical Chemistry, Göttingen, Germany; [3]Department of Experimental Neurodegeneration, Center for Biostructural Imaging of Neurodegeneration; [4]Center for Nanoscale Microscopy and Molecular Physiology of the Brain, University Medical Center Göttingen, University of Göttingen, Göttingen, Germany; [5]Max Planck Institute for Experimental Medicine, Göttingen, Germany; and [6]Department of NMR-Based Structural Biology, Max Planck Institute for Biophysical Chemistry, Göttingen, Germany

ABSTRACT The inherent tendency of proteins to convert from their native states into amyloid aggregates is associated with a range of human disorders, including Alzheimer's and Parkinson's diseases. In that sense, the use of small molecules as probes for the structural and toxic mechanism related to amyloid aggregation has become an active area of research. Compared with other compounds, the structural and molecular basis behind the inhibitory interaction of phthalocyanine tetrasulfonate (PcTS) with proteins such as αS and tau has been well established, contributing to a better understanding of the amyloid aggregation process in these proteins. We present here the structural characterization of the binding of PcTS and its Cu(II) and Zn(II)-loaded forms to the amyloid β-peptide (Aβ) and the impact of these interactions on the peptide amyloid fibril assembly. Elucidation of the PcTS binding modes to Aβ_{40} revealed the involvement of specific aromatic and hydrophobic interactions in the formation of the Aβ_{40}-PcTS complex, ascribed to a binding mode in which the planarity and hydrophobicity of the aromatic ring system in the phthalocyanine act as main structural determinants for the interaction. Our results demonstrated that formation of the Aβ_{40}-PcTS complex does not interfere with the progression of the peptide toward the formation of amyloid fibrils. On the other hand, conjugation of Zn(II) but not Cu(II) at the center of the PcTS macrocyclic ring modified substantially the binding profile of this phthalocyanine to Aβ_{40} and became crucial to reverse the effects of metal-free PcTS on the fibril assembly of the peptide. Overall, our results provide a firm basis to understand the structural rules directing phthalocyanine-protein interactions and their implications on the amyloid fibril assembly of the target proteins; in particular, our results contradict the hypothesis that PcTS might have similar mechanisms of action in slowing the formation of a variety of pathological aggregates.

INTRODUCTION

Neurodegeneration is characterized by the progressive loss of neuronal cells and the decline of motor and cognitive functions (1). Different neuropathological, genetic, and biochemical studies support the role of protein amyloidogenesis in the development of neurodegenerative disorders (2,3). Although their amino acid sequences and the biological environments in which they function have coevolved to maintain peptides and proteins in their soluble states, in some circumstances, they can convert into nonfunctional and potentially damaging protein aggregates (4). A detailed understanding of the mechanism by which proteins of wide structural diversity are transformed into potentially damaging aggregates is therefore of high clinical importance.

Alzheimer's disease (AD) is the most common cause of dementia among neurodegenerative disorders in the elderly population, affecting ~25 million people worldwide (5). Neurodegeneration in AD is characterized by the progressive accumulation of extracellular senile plaques consisting of amyloid β-peptide (Aβ) and intracellular fibrillary tangles consisting of Tau protein (6). The Aβ is a normally secreted, small peptide (39–43 residues) that results from processing of the larger amyloid precursor protein (APP) (7,8). Extensive genetic and cell viability studies

Submitted June 29, 2017, and accepted for publication January 2, 2018.

*Correspondence: cfernan@gwdg.de

Editor: James Shorter.

https://doi.org/10.1016/j.bpj.2018.01.003

support a key role for the Aβ peptide in AD neurodegeneration and oxidative stress (9–11). In its monomeric state, Aβ is best described as an ensemble of structurally heterogeneous conformations, with propensities for β-strand structure at two hydrophobic regions (Leu17–Ala21 and Ile31–Val36), and turn or bend-like structures at the Asp7–Glu11 and Phe20–Ser26 segments (12–14). By contrast, due to the complexity of the structural conversions occurring during the amyloid aggregation process, the mechanism(s) underlying the structural transition from the monomeric Aβ to its aggregated form(s) remains poorly described (4).

Currently, no preventive therapy is available for AD and other protein misfolded diseases (15–17). The ongoing clinical trial strategies for AD include the use of small modified peptides, antibodies, and chemical drugs targeting either Aβ aggregation, clearance, or production (15,16). The continued failures of biomolecules in late clinical trials, including the recent failure of the promising antibody Solanezumab, highlights the urgent need for a better understanding of the aggregation phenomena, its role in the disease progression, and the structural requirements and mechanistic basis of drug candidates. The discovery of small molecules targeting disease-associated protein aggregation is considered one of the most active therapeutic approaches toward neurodegenerative disorders (18). Not only have they been shown to modulate the aggregation of amyloid proteins both in vitro and in vivo, but they also have been used as molecular and structural probes to gain insight into the amyloid aggregation process (19–21). From the screening of large libraries of small compounds, a range of potential candidates with a wide range of chemical structures were found to modulate the aggregation of distinct amyloid proteins (21–34). Notably, poly-aromatic scaffolds belonging to the chemical classes of flavonoids, polyphenols, porphyrins, and phthalocyanines were predominantly identified by these screenings (21–31).

Recently, distinct variants of phthalocyanines and porphyrins have been tested for their ability to impair the amyloid assembly process of proteins linked to neurodegeneration. These molecules are cyclic tetrapyrroles, a class of compounds whose distinguished characteristic is the planarity and hydrophobicity of its aromatic ring system. The phthalocyanine tetrasulfonate (PcTS) compounds are among the most widely investigated tetrapyrroles. The structure of PcTS contains four sulfonic acid groups at the borders of the aromatic rings, whereas the center of the molecule can remain ligand free or coordinated to metal ions of various valences (Fig. S1). Besides the demonstrated prophylactic and therapeutic effects of PcTS in scrapie disease (25,27,35–37), this compound suppressed the filament assembly of αS, a key protein involved in the pathology of Parkinson's disease, leading to the formation of a variety of non-toxic, amorphous αS aggregates (21,38). Interestingly, PcTS was also effective in inhibiting the misfolding and aggregation of vesicle-bound αS (39). The potential of PcTS as an amyloid modulator was also explored on the protein Tau and the Aβ peptide. PcTS was able to interfere with Tau filament assembly by inducing the conversion of the protein into non-toxic soluble oligomers. From a neuroblastoma-cell-based assay, it was demonstrated that PcTS was also an effective modulator of Tau-induced filament formation (40). In the case of the Aβ peptide, it was shown that PcTS was able to induce the clearance of metal-induced toxic Aβ oligomers and their conversion into an amyloid fibrillar meshwork, which coincidentally reduced the toxic activity of Aβ in cellular assays (41). More recently, it was reported that a novel carboxylated Zn(II)-loaded derivative delayed the formation of Aβ oligomers and inhibited Aβ toxicity in neuronal cell lines (42).

Compared with other compounds that show activity as amyloid inhibitors, the structural and molecular basis behind the inhibitory interaction of PcTS with proteins such as αS and Tau has been well established, contributing to a better understanding of the aggregation process in these proteins. In the case of the protein αS, structural characterization of the αS-PcTS complexes indicated that the inhibition of αS amyloid fibril formation in the presence of this compound was a direct consequence of its binding to the N-terminus of the protein (21). The fact that the interaction was shown to be dependent on the presence of the aromatic residues contained in that region demonstrated unequivocally the role of the aromatic moieties as anchoring groups for PcTS binding to αS. These studies revealed also that specific aromatic interaction with the Tyr39 residue provides a central mechanistic basis for the inhibitory process of PcTS on αS fibril formation, whereas the residue-specific structural characterization of the αS-PcTS complex provided the basis for the rational design of non-amyloidogenic species of αS, highlighting the role of aromatic interactions in driving αS amyloid assembly. Added to that, these studies allowed the identification of low-order stacked aggregates of PcTS as the active amyloid inhibitory species (28), whose selective effects on the aromatic moieties in the protein sequence were attributed to their large aromatic surface area.

In the same direction, it was demonstrated that PcTS inhibits the formation of Tau filaments in vitro and in cells by selectively interacting with the aromatic residues Tyr197, Tyr310, Phe346, Phe378, and Tyr394 in the central domain of Tau and converting the protein into soluble oligomers (40). That study revealed also detailed insights into the mechanism of Tau-aggregation inhibition and the structure and dynamics of soluble Tau oligomers, demonstrating that the structure of off-pathway oligomers of Tau is distinct from the structure of toxic Tau oligomers.

The fact that PcTS molecules were shown to block different types of disease-associated protein aggregation, such as that of α-synuclein and Tau proteins, raised the possibility that this compound might have similar structural and molecular mechanisms of action in slowing the formation of a variety of pathological aggregates. In that direction, in this work, we sought to delineate the structural basis of the

interaction of PcTS and metal-loaded variants of this phthalocyanine with Aβ_{40} and to analyze its implications for amyloid fibril formation of the peptide. Elucidation of the PcTS binding modes to Aβ_{40} revealed that both aromatic and hydrophobic interactions play a key role in the process of molecular recognition, ascribed to an interaction mode in which the planarity and hydrophobicity of the aromatic ring system in the phthalocyanine molecule act as main structural determinants for the interaction with Aβ_{40}. In contrast with previous studies on other amyloid proteins, the formation of Aβ_{40}-PcTS complexes did not interfere with the progression of the peptide toward the formation of mature amyloid fibrils. The binding profile of PcTS(Cu(II)) to Aβ_{40} and its effects on the peptide amyloid fibril formation paralleled that of metal-free PcTS. On the other hand, our results demonstrated that conjugation of Zn(II) at the center of the PcTS macrocyclic ring modified substantially the binding profile of this phthalocyanine to Aβ_{40} and became crucial to reverse the effects of metal-free PcTS on the fibril assembly of the peptide. In this case, the coordination geometry preferences of the Zn(II) ion conjugated at the central core of PcTS constituted the key structural factor behind the inhibitory interaction of this phthalocyanine with Aβ_{40}. Overall, the results reported in this work provide a firm basis to understand the structural rules directing phthalocyanine-protein interactions and their implications on the amyloid fibril assembly of the target proteins; in particular, our results contradict the hypothesis that PcTS might have similar mechanisms of action in slowing the formation of a variety of pathological aggregates.

MATERIALS AND METHODS

Sample preparation and reagents

Non-labeled and ^{15}N isotopically enriched Aβ_{40} samples were purchased from EZBiolab (Carmel, IN) and Alexotech (Oslo, Norway), respectively. Peptide samples were prepared according to the alkaline dissolution protocol (12). Lyophilized peptide (1 mg) was dissolved in 400 μL of 10 mM NaOH, incubated for 30 min in ice, aliquoted, and stored at −80°C. Immediately before recording the NMR experiments, one or more Aβ_{40} aliquots were diluted in 20 mM TRIS buffer. The pH was then adjusted to 7.5 and samples were centrifuged at 20,000 × g to eliminate potentially pre-formed aggregates (43). The peptide concentration was measured by ultraviolet spectroscopy using a molar extinction coefficient, $\varepsilon_{280\ nm} = 1490\ cm^{-1}\ M^{-1}$. Purity of the A$\beta_{40}$ solutions was assessed by sodium dodecyl sulfate polyacrylamide gel electrophoresis (SDS-PAGE). PcTS was purchased from MP Biomedicals (Solon, OH); Zn(II) phthalocyanine tetrasulfonic acid (PcTS(Zn(II))) was purchased from Frontier Scientific (Logan, UT); Cu(II) phthalocyanine tetrasulfonic acid (PcTS(Cu(II))) was purchased from Sigma-Aldrich (St. Louis, MO).

Aggregation assay

Aggregation kinetics measurements were performed with 50 μM peptide samples dissolved in 20 mM TRIS buffer at pH 7.5. Samples were incubated at 37°C under constant stirring in the absence and presence of phthalocyanines. Although the Thioflavin T (ThioT) fluorescescence assay is usually used to monitor amyloid fibril formation, in the case of phthalocyanine-treated samples, the reliability of ThioT as an indicator of fibril inhibition may be questionable, since these small molecules interfere significantly and alter ThioT fluorescence in the absence of proteins due to their intrinsic absorbance and fluorescent properties (44). Accordingly, in this work, we used an NMR-based approach that measures the consumption of the monomeric state of the amyloid protein/peptide during the progression of the aggregation process (21,45,46). The amount of soluble Aβ monomers at different time points of the aggregation assay was determined by integration of the protein NMR resonances in the aliphatic region of the one-dimensional (1D) ^{1}H NMR spectrum (0.7–1.0 ppm). Aggregation yields were normalized to the initial values of the free Aβ peptide sample as previously described (45). Endpoint aliquots of aggregation assays were loaded in 8–23% gradient SDS-PAGE (47) and were visualized using a silver staining protocol as previously described (48).

NMR spectroscopy

NMR spectra were acquired on a 600 MHz Avance III (Bruker, Billerica, MA) equipped with a cryogenically cooled triple-resonance ^{1}H(^{13}C/^{15}N) TCI probe. Heteronuclear NMR experiments were performed with pulsed-field-gradient-enhanced pulse sequences on 100 μM ^{15}N-labeled peptide samples in 20 mM TRIS buffer (pH 7.5) at 15°C. 1D ^{1}H-NMR experiments were acquired at 15°C on 50 μM unlabeled Aβ_{40} dissolved in deuterated 20 mM TRIS buffer (pH 7.5). Aggregation did not occur under these low temperature conditions and absence of stirring.

For the mapping experiments, ^{1}H-^{15}N heteronuclear single quantum correlation (HSQC) amide cross-peaks affected during PcTS titration were identified by comparing their intensities (I) with those of the same cross-peaks in the data set of samples lacking the tetrapyrrolic compound (I_0) (49). Mean weighted chemical-shift displacements (^{1}H-^{15}N MWCS) were calculated as $[(\Delta\delta^1H)^2 + (\Delta\delta^{15}N)^2/25]^{1/2}$ (49).

Pulsed-field-gradient-NMR experiments were acquired at 15°C on 100 μM unlabeled Aβ_{40} peptide samples dissolved in D_2O and containing dioxane as an internal radius standard and viscosity probe. NMR spectra were recorded in the absence and presence of phthalocyanines. A series of 20 1D spectra were collected as a function of gradient amplitude. The gradient strength was shifted from 0.68 to 32 G cm^{-1} in a linear manner.

Acquisition, processing, and visualization of the spectra were performed by using TOPSPIN 2.0 (Bruker) and Sparky (Goddard and Kelner, University of California San Francisco).

Electron microscopy

Ten-microliter aliquots withdrawn from aggregation reactions were adsorbed onto Formvar/carbon-coated copper grids (Pella, Redding, CA) and negative stained with 2% (w/v) uranyl acetate. Images were obtained at various magnifications (1000–90,000×) using a Philips CM120 transmission electron microscope.

RESULTS

PcTS is not able to impair Aβ_{40} amyloid fibril assembly

The ability of PcTS to interfere with Aβ_{40} amyloid assembly was analyzed by using NMR, SDS-PAGE, and transmission electron microscopy (TEM). As shown in Fig. 1, *A* and *B*, the time course of aggregation of free Aβ_{40} monitored as monomer consumption by 1D ^{1}H-NMR spectroscopy was comparable to that measured in the presence of PcTS. Indeed, we found that PcTS did not reduce the amount of

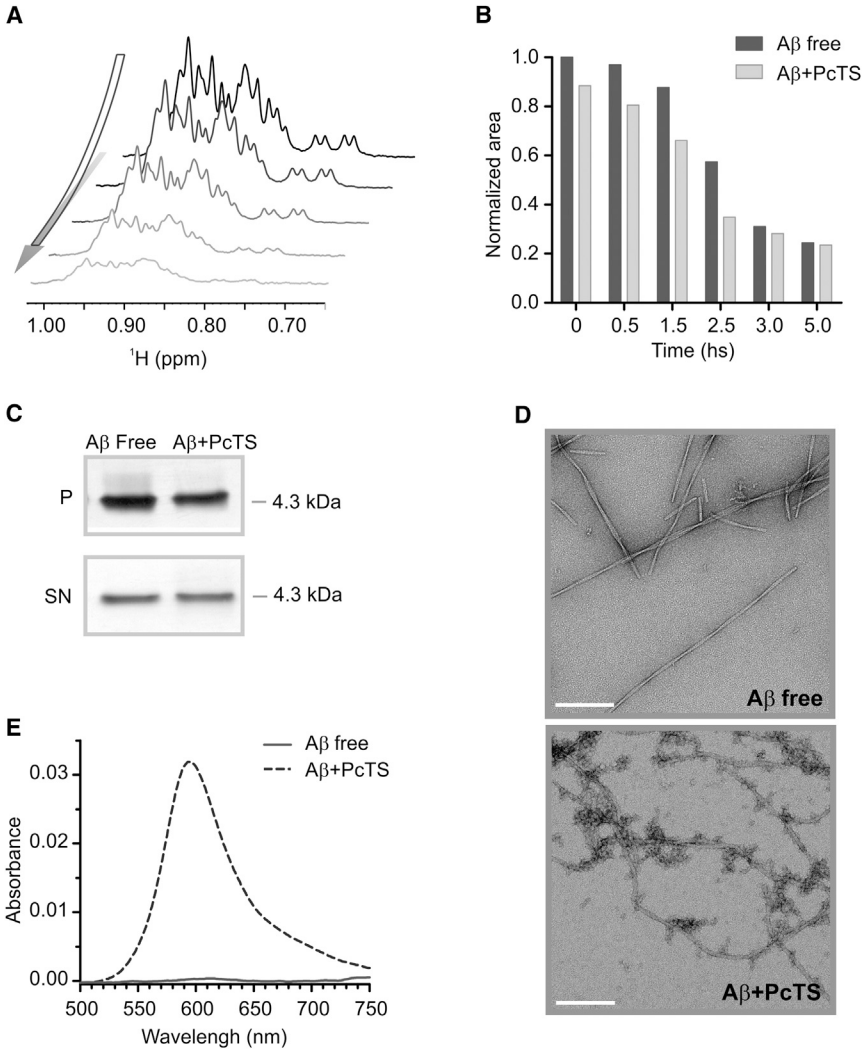

FIGURE 1 Analysis of PcTS effects on Aβ_{40} amyloid fibril formation. (*A*) 1D ^{1}H-NMR spectra (aliphatic region) of 50 μM Aβ_{40} as a function of aggregation time. Monomer consumption was quantified by integration of the NMR signals in the 0.7–1.0 ppm spectral region. (*B*) Level of remaining soluble Aβ_{40} monomers in the absence (*black bars*) and presence (*gray bars*) of 150 μM PcTS, determined by 1D ^{1}H-NMR spectroscopy. (*C*) SDS-PAGE of Aβ_{40} peptide soluble (SN) and insoluble (P) fractions of the end points of the aggregation assays (50 μM Aβ_{40}) in the absence (control) and presence of 150 μM PcTS. (*D*) Representative negative-stain electron microscopy images of Aβ_{40} aggregates (50 μM Aβ_{40} samples) generated in the absence and presence of 150 μM PcTS. Scale bars, 100 nm. (*E*) Electronic absorption spectra corresponding to the pellet fraction of 50 μM Aβ_{40} aggregations obtained in the absence (*solid line*) or presence (*dashed line*) of 150 μM PcTS.

aggregated Aβ_{40} (Fig. 1 *C*). When the final product of aggregation of Aβ_{40} in PcTS-treated samples was analyzed by TEM, the images revealed the presence of amyloid fibrils decorated with a variety of small, apparently amorphous species (Fig. 1 *D*). Consistent with this, absorption spectroscopy on extensively washed Aβ_{40} aggregates from PcTS-treated samples indicated that PcTS molecules were incorporated into the Aβ_{40} amyloid fibrils (Fig. 1 *E*). Altogether, the results demonstrate that even though PcTS appears to be efficiently incorporated into the final product of aggregation of Aβ_{40}, the cyclic tetrapyrrole does not inhibit the amyloid fibril formation of the peptide.

Formation of the Aβ_{40}-PcTS complex at the N- and C-termini is mediated by aromatic and hydrophobic interactions

To assess whether the absence of an inhibitory effect of PcTS on Aβ_{40} amyloid assembly might be linked to the lack of interaction of the cyclic tetrapyrrole with monomeric Aβ_{40}, we used ^{1}H-^{15}N HSQC spectra. The central region of the ^{1}H-^{15}N HSQC spectrum of a 100 μM sample of uniformly ^{15}N-labeled Aβ_{40} recorded in 20 mM TRIS buffer (pH 7.5) at 15°C is shown in Fig. 2 *A*.

The resonances were well resolved and sharp, with a limited dispersion of chemical shifts, reflecting the disordered nature and the high degree of mobility of the backbone that characterize the monomeric state of Aβ_{40} peptide. Upon titration of ^{15}N-enriched Aβ_{40} with increasing concentrations of PcTS, the ^{1}H-^{15}N HSQC spectra demonstrated measurable broadening and chemical-shift changes in a discrete number of residues distributed throughout the peptide sequence (Fig. 2, *A* and *B*). This behavior indicates that a certain number of signals from free and bound states of Aβ_{40} cannot be resolved and are averaged in a manner that leads to resonance line broadening, indicative of a system undergoing intermediate exchange on the NMR timescale. In other words, the broadening is caused by an exchange of Aβ_{40} molecules between the free and PcTS-bound states, as previously reported for the αS and

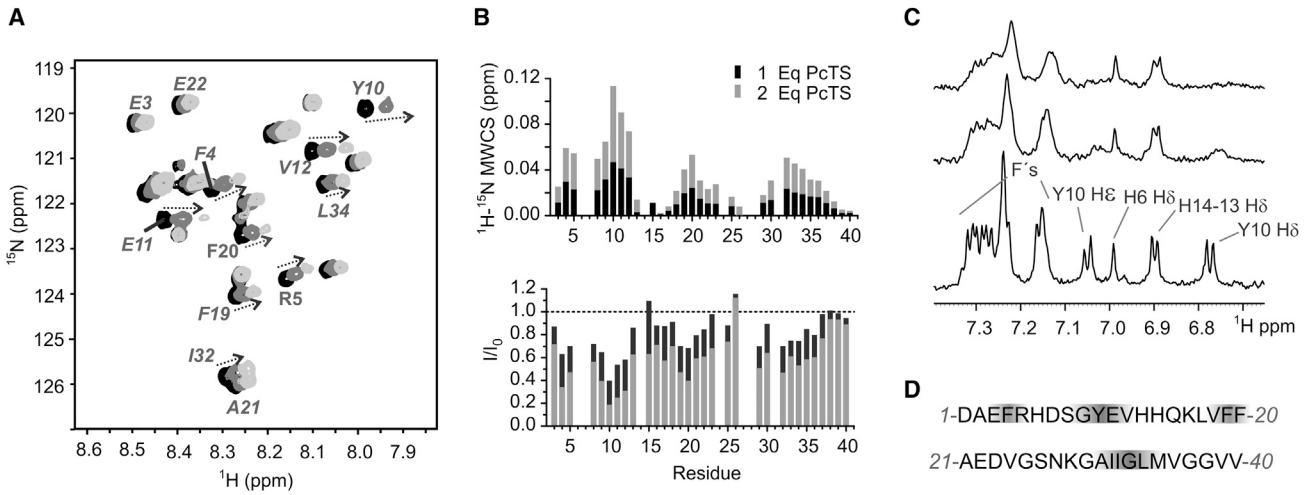

FIGURE 2 Analysis of PcTS binding to Aβ_{40} by NMR. (*A*) Overlaid ^{1}H-^{15}N HSQC spectra of 100 μM Aβ_{40} in the absence (*black*) and presence (*dark gray*) of 100 and 200 μM PcTS (*gray*). Amino acid residues broadened significantly or beyond detection are identified. (*B*) I/I$_0$ profiles and differences in the mean-weighted chemical-shift displacements (^{1}H-^{15}N MWCS) of the backbone amide groups of 100 μM Aβ_{40} in the presence of 100 μM (*black*) and 200 μM PcTS (*gray*). (*C*) 1D ^{1}H-NMR of aromatic side chains of 50 μM Aβ_{40} in the absence (*lower trace*) and presence of 12.5 μM (*middle trace*) and 25 μM PcTS (*upper trace*). The slight effects observed on His13 and His14 upon addition of PcTS are likely due to its proximity to Tyr10. (*D*) Primary sequence of Aβ_{40} indicating in gray the identified PcTS binding regions.

Tau proteins (21,28,40). The effects became evident at 100 μM PcTS and the broadening of resonances was further pronounced at 200 μM PcTS. A detailed analysis of ^{1}H-^{15}N backbone amide signals allowed us to identify four major binding interfaces for PcTS in Aβ_{40}: aa3–5, 8–12, 18–23, and 32–37 (Fig. 2 *B*), as reflected by the intensities and chemical-shift interaction profiles. A close analysis of the cross-peaks exhibiting severe broadening effects and chemical-shift displacements upon titration with PcTS revealed that they correspond to regions located in the proximity of aromatic residues (Phe in position 4, Tyr in position 10, and two Phes in positions 19 and 20) and to a hydrophobic segment at the C-terminus (Fig. 2, *B* and *D*).

Considering that the degree of perturbation observed on the backbone amide groups of Aβ_{40} in the presence of the PcTS compound might be influenced also by the occurrence of other structural events, such as solvent-exchange phenomena triggered by the ligand-peptide interaction, to probe further the role of aromatic residues in the Aβ_{40}-PcTS interaction, we conducted NMR experiments aimed to directly detect the resonances of the aromatic side chains of Aβ_{40}. The 1D ^{1}H-NMR spectrum of Aβ_{40} shows well-resolved clusters of resonances in the 6.5–7.5 ppm range, comprising the side chains of different aromatic residues: Phe4, His6, Tyr10, His13, His14, Phe19, and Phe20 (Fig. 2 *C*). The distribution of these residues throughout the Aβ_{40} sequence provides excellent probes for exploring the binding features of the PcTS ligand to the peptide. Clearly, the binding features observed for PcTS confirm the direct role played by the aromatic side chains of Tyr10 of Aβ_{40} in the interaction process (Fig. 2 *C*). Although complicated by severe signal overlapping, the broadening effects induced by PcTS on the cluster of resonances assigned to Phe residues at positions 4, 19, and 20 became also evident. Interestingly, the titration experiments showed only small perturbations caused by PcTS on the resonances assigned to the imidazole rings of histidines at positions 6, 13, and 14, likely due to the proximity of these residues to Phe4 and Tyr10, suggesting a lack of interaction of the phthalocyanine with the imidazole rings at these sites.

To assess further the assembly state of the Aβ_{40} peptide in the absence and presence of PcTS, we performed pulsed-field gradient NMR experiments. Pulsed-field gradient NMR on the free and PcTS-complexed states of the Aβ_{40} peptide showed identical decay curves of NMR signal intensity (Fig. S2). The results obtained from the curves showed that the free Aβ_{40} and its PcTS-complexed form have the same apparent diffusion coefficient of 1.08×10^{-8} cm^2 s^{-1} at 15°C and thus the same assembly state. A calculated hydrodynamic radius of ~1.5 nm demonstrates that the NMR-visible states of the peptide are mainly monomeric, in good agreement with previous reports of the hydrodynamic properties of monomeric Aβ_{40} peptide (50). Added to that, the absence of noticeable changes in the hydrodynamic properties of the Aβ_{40} peptide upon addition of PcTS (Fig. S2) indicates that the binding of the phthalocyanine to monomeric Aβ_{40} would proceed via low-order stacked species of the compound, as previously reported for the interactions of PcTS with the protein α-synuclein (28). These results allow us to conclude that 1) PcTS binds to the monomeric form of Aβ_{40}; 2) both N- and C-terminal regions of Aβ_{40} represent binding interfaces for PcTS, ascribed to an interaction mode in which the planarity and hydrophobicity of the aromatic ring system in the

phthalocyanine molecule act as main structural determinants for the interaction with Aβ_{40}; 3) Phe4, Tyr10, Phe at positions 19 and 20, and residues 32–37 constitute the main anchoring groups for PcTS binding to Aβ_{40}, whereas no direct interaction was observed with the cluster of histidines in positions 6, 13, and 14; and 4) formation of Aβ_{40}-PcTS complexes does not interfere with the progression of the peptide toward the formation of mature amyloid fibrils.

PcTS(Zn(II)) but not PcTS(Cu(II)) inhibits amyloid fibril formation of Aβ_{40}

It is well documented that the incorporation of different metal cations into the central core of phthalocyanines strongly influences the biological activity of this type of molecule (27,28,36,37,51–54). Consistent with evidence that relates Cu(II) and Zn(II) to the etiology of AD (55,56), we decided to evaluate the effects of the Cu(II)- and Zn(II)-bound forms of PcTS on Aβ_{40} amyloid fibril assembly (Fig. 3, *A–D*). Our TEM studies showed that the PcTS(Zn(II)) derivative completely abolished Aβ_{40} amyloid fibril formation, inducing a variety of small, amorphous, non-fibrillar Aβ_{40} aggregates (Fig. 3 *B*), whereas PcTS(Cu(II))-treated samples showed an amyloid fibril morphology similar to those of free Aβ_{40} samples (Fig. S3). Interestingly, Fig. 3 *C* shows that Aβ_{40} monomers are rapidly assembled into non-detectable NMR species upon addition of PcTS(Zn(II)), suggesting that PcTS(Zn(II))-treated samples became predominantly populated by an aggregated Aβ_{40} state(s). As shown in Fig. 3 *D*, analysis of the final product of aggregated Aβ_{40}-PcTS(Zn(II)) samples, performed by SDS-PAGE, confirm this finding. As observed for the PcTS-treated Aβ_{40} samples, absorption spectroscopy on extensively washed Aβ_{40} aggregates from PcTS(Zn(II))-treated samples indicates that this compound is incorporated into the Aβ_{40} aggregates (Fig. S4). In addition, the observation of the characteristic PcTS(Zn(II)) electronic spectrum in the pellet fraction of the Aβ_{40} aggregates demonstrates conclusively that the metal ion remains coordinated to the tetrapyrrolic macrocycle under these experimental conditions. On the other hand, incubation of Aβ_{40} samples in the presence of PcTS(Cu(II)) resulted in SDS-PAGE profiles similar to that observed for metal-free PcTS (Fig. S3). Overall, these results demonstrate that coordination of Zn(II), but not Cu(II), into the PcTS scaffold renders phthalocyanine an efficient modulator of Aβ_{40} amyloid fibril formation.

PcTS(Zn(II)) binds preferentially to the N-terminal histidine residues of Aβ_{40}

To evaluate the possibility that the distinct effects of PcTS(Zn(II)) and PcTS(Cu(II)) on Aβ_{40} fibril formation correlate with the features of their binding to the peptide, we analyzed the interaction profiles of both ligands with

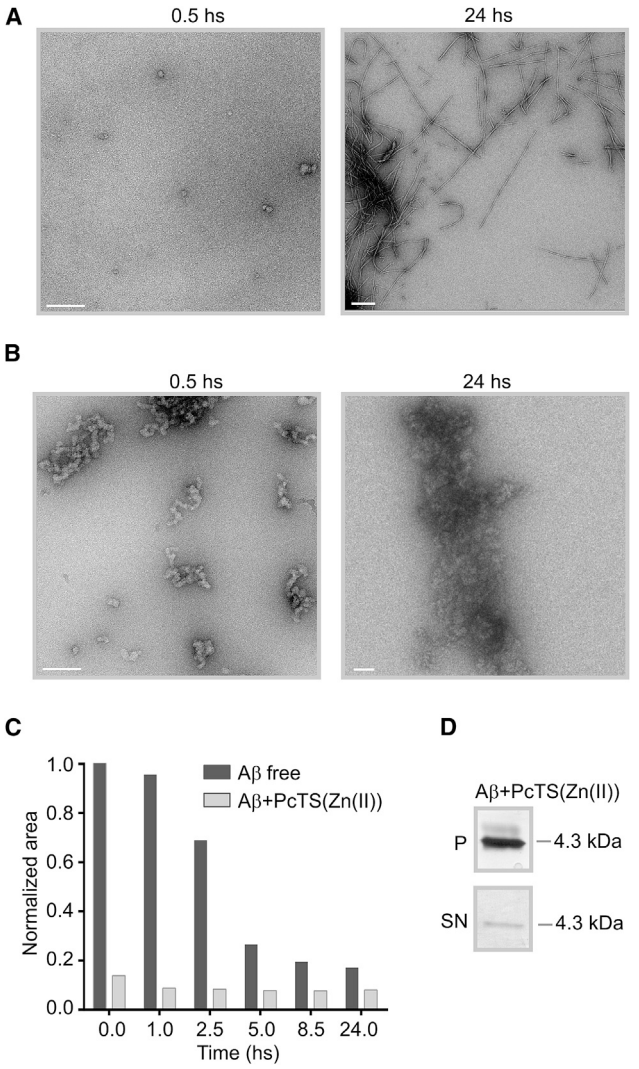

FIGURE 3 Analysis of PcTS(Zn(II)) effects on Aβ_{40} amyloid assembly. (*A* and *B*) Representative negative-stain EM images of Aβ_{40} aggregates (50 μM Aβ_{40} samples) generated in the absence (*A*) and presence of 150 μM PcTS(Zn(II)) (*B*). The products of aggregation were analyzed at the time intervals of 0.5 and 24 h of the aggregation assay. Scale bars, 100 nm. (*C*) Level of remaining soluble Aβ_{40} monomers in the absence (*black bars*) and presence (*gray bars*) of 150 μM PcTS(Zn(II)) determined by 1D ^{1}H-NMR spectroscopy during the time course of the aggregation assay. (*D*) SDS-PAGE analysis of Aβ_{40} peptide soluble (SN) and insoluble (P) fractions of the end point of the aggregation assays in the presence of three equivalents of PcTS(Zn(II)).

monomeric Aβ_{40}. To this purpose, we first used 1D ^{1}H-NMR spectroscopy by monitoring again the spectral region containing the resonances of aromatic side chains in Aβ_{40}. Whereas the binding features of PcTS(Cu(II)) to Aβ_{40} resemble those described for the metal-free phthalocyanine (Fig. 4 *A*), the interaction profile of PcTS(Zn(II)) changed substantially, suggesting a role for the imidazole rings of histidine residues at positions 6, 13, and 14 of Aβ_{40} as the main anchoring groups for PcTS(Zn(II)) binding. As reported for the interaction with metal-free PcTS,

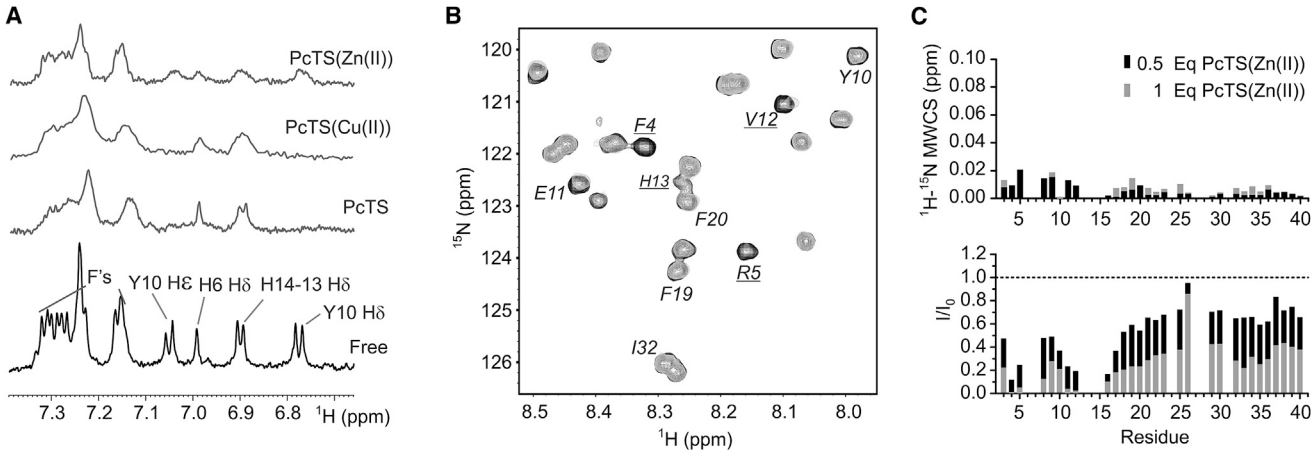

FIGURE 4 Analysis of PcTS(Zn(II)) binding to Aβ_{40} by NMR. (*A*) 1D ^{1}H-NMR of aromatic side chains of 50 μM Aβ_{40} in the absence (*lower trace*) and presence of 25 μM of PcTS and its Zn(II) and Cu(II) derivatives. The higher degree of signal broadening in the spectrum of the Aβ_{40}-PcTS(Cu(II)) complex obeys the paramagnetic nature of Cu(II) ions. Spectra were registered at 15°C in deuterated 20 mM TRIS$_d$ buffer (pH 7.5). (*B*) Overlaid ^{1}H-^{15}N HSQC spectra of 100 μM Aβ_{40} in the absence (*black*) and presence (*gray*) of 50 μM PcTS(Zn(II)). Amino acid residues broadened significantly or beyond detection are underlined. (*C*) I/I$_0$ profiles and differences in the mean-weighted chemical-shift displacements of the backbone amide groups of 100 μM Aβ_{40} in the presence of 50 μM (*black*) and 100 μM PcTS(Zn(II)) (*gray*).

the hydrodynamic properties of Aβ_{40} remained unchanged upon complexation with PcTS(Cu(II)) and PcTS(Zn(II)) (data not shown).

To gain further insight into the unique binding properties of PcTS(Zn(II)) to Aβ_{40}, we then used ^{1}H-^{15}N HSQC spectroscopy (Fig. 4 *B*). Titration of Aβ_{40} samples with 50–100 μM PcTS(Zn(II)) caused a severe broadening, in some cases beyond detection, of a group of resonances centered at the His6 and His13-14 sites (Fig. 4 *C*). Thus, the combined analysis of 1D and 2D NMR titration experiments confirm that the imidazole rings of histidines at positions 6, 13, and 14 constitute the main anchoring groups for PcTS(Zn(II)) binding to Aβ_{40}. Added to the major effects centered on the resonances of His residues, the binding of PcTS(Zn(II)) to Aβ_{40} causes a significant and general signal attenuation phenomenon. The general signal intensity reduction in the NMR spectra due to PcTS(Zn(II)) binding is consistent with the picture obtained by TEM and SDS-PAGE analysis, demonstrating that upon complexation with PcTS(Zn(II)), the Aβ_{40} samples become mostly populated by an aggregated, non-fibrillar state(s).

DISCUSSION

The discovery and design of small molecules that efficiently target disease-associated protein aggregation became a promising tool for the development of therapeutic strategies. To understand fully, from a mechanistic perspective, the way these compounds might modulate protein aggregation, it is of paramount importance to decipher the structural and molecular basis of the implied protein-ligand interactions, but also to investigate the structural requirements of the small molecules that are critical for efficient and specific anti-amyloid activity.

In this work, we have delineated the structural basis for the interaction of PcTS with Aβ_{40} and demonstrated that the nature of the metal ion incorporated into the heterocycle center modulates the binding features and the activity of PcTS on Aβ_{40} amyloid fibril formation. The NMR analysis of Aβ_{40} complexes with PcTS demonstrated unequivocally the role of the aromatic moieties as anchoring groups for PcTS binding to the monomeric state of Aβ_{40}, ascribed to a binding mode in which the planarity and hydrophobicity of the aromatic ring system in the phthalocyanine molecule act as main structural determinants for the interaction with Aβ_{40}.

Our studies revealed also that hydrophobic interactions between the macrocycle ring of PcTS and the central and C-terminal hydrophobic clusters of Aβ_{40} contribute strongly to the binding process. Electrostatic interactions between negative sulfonates at the periphery of the aromatic ring in PcTS and suitably positioned positive centers, likely provided by the lysine and arginine residues located in the vicinity of the binding sites, might also have an auxiliary role as modulators of the interaction. Overall, the interaction scenario described here for Aβ_{40}-PcTS seems to be a unique feature of this complex, since only aromatic interactions were proposed to mediate the inhibitory binding of PcTS to the proteins αS and Tau (21,40). Interestingly, these differences might provide a structural explanation for the lack of inhibitory activity of PcTS molecules against Aβ_{40} amyloid fibril formation. The central and C-terminal hydrophobic segments that were strongly affected by PcTS binding to monomeric Aβ_{40} constitute the two main β-sheet segments that characterize the architecture of Aβ fibrils (57,58). Intramolecularly, the β-sheets are held together by hydrophobic interactions, and several works indicate that the proximity of the N- and C-terminal parts of the Aβ sequence would be pre-ordered at the oligomeric and

monomeric levels as well (12–14,59), where the central and C-terminal hydrophobic segments might form a common binding interface, of a transient nature, capable of interacting with the hydrophobic PcTS species. Accommodation of the macrocycle ring of PcTS molecules into that transient hydrophobic interface would act then by enhancing or stabilizing rather than compromising early intra- and intermolecular interactions necessary for amyloid structural transitions. Added to the lack of inhibitory effects on Aβ_{40} amyloid fibril assembly, the fact that PcTS molecules appear mostly incorporated into Aβ_{40} aggregates gives further support to this hypothesis.

Since it was demonstrated that the conjugation of metal ions into the central cavity of phthalocyanines influences the self-association propensity and the biological activity of these compounds, we then extended our studies to Zn(II) and Cu(II)-loaded phthalocyanines. Our study revealed that metal incorporation into the architecture of PcTS influenced the activity of these compounds on Aβ_{40} amyloid fibril assembly in different ways. Conjugation with Zn(II) resulted in a PcTS variant with inhibitory effects on Aβ_{40} amyloid fibril formation. We found that PcTS(Zn(II)) produced a variety of small, apparently amorphous, non-fibrillar Aβ_{40} aggregates. On the other hand, the Aβ_{40} aggregates in the PcTS(Cu(II))-treated samples showed an amyloid morphology comparable with that of free Aβ_{40} samples.

Considering that the phthalocyanines studied in our work exist in solution mostly as self-stacked aggregates (28,60), the differences observed in their activity against Aβ_{40} fibril formation seems to be relatively insensitive to the tendencies of PcTS derivatives to self-associate. Interestingly, another metal-sensitive property of PcTS molecules that might influence their binding features and consequently their activity as amyloid inhibitors is related to the different properties of the metal ion coordinated into the core aromatic ring of the phthalocyanine. Indeed, the residual positive charge located at the metal ion, the preferred coordination stereochemistry of the metal ion, or its relative affinity for axial ligands might potentially act as critical structural determinants for the mode(s) of interaction of these compounds with protein target sites. In that sense, we noticed that coordination of Zn(II) to PcTS redirected the binding preferences of the molecule toward the N-terminal region, where the interaction was mostly centered on the histidine residues located at that region. It is well established that zinc binds to the same three His residues as copper, with K_{dapp} of ~0.1 μM for Cu(II) and ~2 μM for Zn(II) ions (55,56). However, when loaded into the central cavity of PcTS, only Zn(II) ions, not Cu(II), might be still able to accommodate histidine(s) into its coordination environment, likely reflecting a higher capability for the Zn(II)-metallated species to accommodate axial ligands out of the plane of the PcTS scaffold. Although more work is needed to confirm this hypothesis, this interpretation is in agreement with the more pronounced propensity of Zn(II) ions to form flexible and open coordination geometries. Overall, these results indicate that the nature of the metal ion conjugated at the center of the phthalocyanine ring may modulate the binding features and anti-amyloid activity of the PcTS compound by targeting other binding sites in the Aβ_{40} peptide.

Related to the molecular events behind the effects of PcTS(Zn(II)) on Aβ_{40} amyloid fibril formation, it was shown that the N-terminal hydrophilic region of the free Aβ adopts an extended conformation rich in PII helix that is proposed to be essential to keep the peptide soluble and protected from amorphous aggregation (61,62). Thus, we assume that the presence of the Zn(II)-loaded phthalocyanine might perturb the structural preferences at the N-terminal hydrophilic region by inducing the formation of a network of Aβ peptides, in which the metal ion conjugated to the PcTS molecule would act to stabilize these structures by binding histidines belonging to adjacent peptides. Indeed, previous works demonstrated that Zn(II) ions can bridge intermolecular N-terminus interaction of the type Nτ-Zn(II)-Nτ between histidine imidazole rings of different Aβ polypeptide chains, preventing the structural transitions of the peptide into amyloid-competent species (63,64). In that direction, recent studies focused on the interaction of heme centers with Aβ amyloid confirmed the binding of the heme iron to the His residues in the N-terminal region of the peptide and indicated that this interaction was crucial to prevent the formation of Aβ ordered fibrils through a mechanism that involved Fe(III)-mediated intermolecular histidine bridging (65,66).

Added to the fact that cyclic tetrapyrroles have been shown to block different types of disease-associated protein aggregation, the previous studies of the effects of PcTS on α-synuclein and Tau proteins raised the possibility that this compound might have similar mechanisms of action in slowing the formation of a variety of pathological aggregates. However, based on the fact that PcTS was not able to impair the amyloid fibril formation of Aβ_{40}, our work seems to contradict that hypothesis. Although more work is clearly needed, these results likely reflect the differences in the universe of structural conversions and driving forces that direct the amyloid aggregation of these proteins.

Overall, the results reported in this work provide a firm basis to understand the structural rules directing phthalocyanine-protein interactions and their implications for the amyloid fibril assembly of the target protein. Because the structural basis for the anti-amyloid effects of these molecules is starting to emerge, combined efforts from the fields of structural and cell biology are needed at this stage to elucidate the precise molecular mechanism(s) of action of these molecules.

SUPPORTING MATERIAL

Four figures are available at http://www.biophysj.org/biophysj/supplemental/S0006-3495(18)30066-3.

AUTHOR CONTRIBUTIONS

A.A.V.-G. and C.O.F. designed research. A.A.V.-G. and D.R. performed research. A.A.V.-G., T.F.O., M.A.M.-M., C.G., and C.O.F analyzed data and wrote the article.

ACKNOWLEDGMENTS

A.A.V.-G. thanks Gudrun Heim for helpful assistance during the transmission electron microscopy measurements.

C.O.F. thanks Universidad Nacional de Rosario, Agencia Nacional de Promoción Científica y Tecnológica, Fondo para la Investigación Científica y Tecnológica, Fundacion Medife, and the Alexander von Humboldt Foundation for financial support. C.O.F. and C.G. thank the Max Planck Society for support. T.F.O. is supported by the Deutsche Forschungsgemeinschaft Center for Nanoscale Microscopy and Molecular Physiology of the Brain (CNMPB).

REFERENCES

1. Luheshi, L. M., D. C. Crowther, and C. M. Dobson. 2008. Protein misfolding and disease: from the test tube to the organism. *Curr. Opin. Chem. Biol.* 12:25–31.
2. Soto, C. 2003. Unfolding the role of protein misfolding in neurodegenerative diseases. *Nat. Rev. Neurosci.* 4:49–60.
3. Chiti, F., and C. M. Dobson. 2006. Protein misfolding, functional amyloid, and human disease. *Annu. Rev. Biochem.* 75:333–366.
4. Chiti, F., and C. M. Dobson. 2017. Protein misfolding, amyloid formation, and human disease: a summary of progress over the last decade. *Annu. Rev. Biochem.* 86:27–68.
5. Thies, W., L. Bleiler; Alzheimer's Asssociation. 2013. 2013 Alzheimer's disease facts and figures. *Alzheimers Dement.* 9:208–245.
6. Hardy, J., and D. J. Selkoe. 2002. The amyloid hypothesis of Alzheimer's disease: progress and problems on the road to therapeutics. *Science.* 297:353–356.
7. Fraser, P. E., L. Lévesque, and D. R. McLachlan. 1993. Biochemistry of Alzheimer's disease amyloid plaques. *Clin. Biochem.* 26:339–349.
8. Checler, F. 1995. Processing of the β-amyloid precursor protein and its regulation in Alzheimer's disease. *J. Neurochem.* 65:1431–1444.
9. Ashe, K. H., and K. R. Zahs. 2010. Probing the biology of Alzheimer's disease in mice. *Neuron.* 66:631–645.
10. Chauhan, V., and A. Chauhan. 2006. Oxidative stress in Alzheimer's disease. *Pathophysiology.* 13:195–208.
11. Jonsson, T., J. K. Atwal, …, K. Stefansson. 2012. A mutation in APP protects against Alzheimer's disease and age-related cognitive decline. *Nature.* 488:96–99.
12. Hou, L., H. Shao, …, M. G. Zagorski. 2004. Solution NMR studies of the Aβ(1–40) and Aβ(1–42) peptides establish that the Met35 oxidation state affects the mechanism of amyloid formation. *J. Am. Chem. Soc.* 126:1992–2005.
13. Wang, C. 2011. Solution NMR studies of Aβ monomer dynamics. *Protein Pept. Lett.* 18:354–361.
14. Sgourakis, N. G., Y. Yan, …, A. E. Garcia. 2007. The Alzheimer's peptides Aβ40 and 42 adopt distinct conformations in water: a combined MD/NMR study. *J. Mol. Biol.* 368:1448–1457.
15. Mangialasche, F., A. Solomon, …, M. Kivipelto. 2010. Alzheimer's disease: clinical trials and drug development. *Lancet Neurol.* 9:702–716.
16. Schneider, L. S., F. Mangialasche, …, M. Kivipelto. 2014. Clinical trials and late-stage drug development for Alzheimer's disease: an appraisal from 1984 to 2014. *J. Intern. Med.* 275:251–283.
17. Bachurin, S. O., E. V. Bovina, and A. A. Ustyugov. 2017. Drugs in clinical trials for Alzheimer's disease: the major trends. *Med. Res. Rev.* 37:1186–1225.
18. Liu, T., and G. Bitan. 2012. Modulating self-assembly of amyloidogenic proteins as a therapeutic approach for neurodegenerative diseases: strategies and mechanisms. *ChemMedChem.* 7:359–374.
19. Villemagne, V. L., V. Doré, …, C. C. Rowe. 2017. Aβ-amyloid and tau imaging in dementia. *Semin. Nucl. Med.* 47:75–88.
20. Arja, K., D. Sjölander, …, K. P. Nilsson. 2013. Enhanced fluorescent assignment of protein aggregates by an oligothiophene-porphyrin-based amyloid ligand. *Macromol. Rapid Commun.* 34:723–730.
21. Lamberto, G. R., A. Binolfi, …, C. O. Fernández. 2009. Structural and mechanistic basis behind the inhibitory interaction of PcTS on α-synuclein amyloid fibril formation. *Proc. Natl. Acad. Sci. USA.* 106:21057–21062.
22. Bulic, B., M. Pickhardt, …, E. Mandelkow. 2009. Development of tau aggregation inhibitors for Alzheimer's disease. *Angew. Chem. Int. Ed. Engl.* 48:1740–1752.
23. Schenk, D., G. S. Basi, and M. N. Pangalos. 2012. Treatment strategies targeting amyloid β-protein. *Cold Spring Harb. Perspect. Med.* 2:a006387.
24. Masuda, M., N. Suzuki, …, M. Hasegawa. 2006. Small molecule inhibitors of α-synuclein filament assembly. *Biochemistry.* 45:6085–6094.
25. Caughey, B., W. S. Caughey, …, J. D. Morrey. 2006. Prions and transmissible spongiform encephalopathy (TSE) chemotherapeutics: a common mechanism for anti-TSE compounds? *Acc. Chem. Res.* 39:646–653.
26. Ehrnhoefer, D. E., J. Bieschke, …, E. E. Wanker. 2008. EGCG redirects amyloidogenic polypeptides into unstructured, off-pathway oligomers. *Nat. Struct. Mol. Biol.* 15:558–566.
27. Caughey, W. S., S. A. Priola, …, B. Caughey. 2007. Cyclic tetrapyrrole sulfonation, metals, and oligomerization in antiprion activity. *Antimicrob. Agents Chemother.* 51:3887–3894.
28. Lamberto, G. R., V. Torres-Monserrat, …, C. O. Fernández. 2011. Toward the discovery of effective polycyclic inhibitors of α-synuclein amyloid assembly. *J. Biol. Chem.* 286:32036–32044.
29. Wagner, J., S. Krauss, …, M. Fuhrmann. 2015. Reducing tau aggregates with anle138b delays disease progression in a mouse model of tauopathies. *Acta Neuropathol.* 130:619–631.
30. Wagner, J., S. Ryazanov, …, A. Giese. 2013. Anle138b: a novel oligomer modulator for disease-modifying therapy of neurodegenerative diseases such as prion and Parkinson's disease. *Acta Neuropathol.* 125:795–813.
31. Levin, J., F. Schmidt, …, A. Giese. 2014. The oligomer modulator anle138b inhibits disease progression in a Parkinson mouse model even with treatment started after disease onset. *Acta Neuropathol.* 127:779–780.
32. Scherzer-Attali, R., R. Shaltiel-Karyo, …, E. Gazit. 2012. Generic inhibition of amyloidogenic proteins by two naphthoquinone-tryptophan hybrid molecules. *Proteins.* 80:1962–1973.
33. Frydman-Marom, A., R. Shaltiel-Karyo, …, E. Gazit. 2011. The generic amyloid formation inhibition effect of a designed small aromatic β-breaking peptide. *Amyloid.* 18:119–127.
34. Frydman-Marom, A., M. Rechter, …, E. Gazit. 2009. Cognitive-performance recovery of Alzheimer's disease model mice by modulation of early soluble amyloidal assemblies. *Angew. Chem. Int. Ed. Engl.* 48:1981–1986.
35. Caughey, B., and P. T. Lansbury. 2003. Protofibrils, pores, fibrils, and neurodegeneration: separating the responsible protein aggregates from the innocent bystanders. *Annu. Rev. Neurosci.* 26:267–298.
36. Caughey, W. S., L. D. Raymond, …, B. Caughey. 1998. Inhibition of protease-resistant prion protein formation by porphyrins and phthalocyanines. *Proc. Natl. Acad. Sci. USA.* 95:12117–12122.
37. Priola, S. A., A. Raines, and W. S. Caughey. 2000. Porphyrin and phthalocyanine antiscrapie compounds. *Science.* 287:1503–1506.

38. Lee, E. N., H. J. Cho, …, S. R. Paik. 2004. Phthalocyanine tetrasulfonates affect the amyloid formation and cytotoxicity of α-synuclein. *Biochemistry.* 43:3704–3715.

39. Fonseca-Ornelas, L., S. E. Eisbach, …, M. Zweckstetter. 2014. Small molecule-mediated stabilization of vesicle-associated helical α-synuclein inhibits pathogenic misfolding and aggregation. *Nat. Commun.* 5:5857.

40. Akoury, E., M. Gajda, …, M. Zweckstetter. 2013. Inhibition of tau filament formation by conformational modulation. *J. Am. Chem. Soc.* 135:2853–2862.

41. Park, J. W., J. S. Ahn, …, S. R. Paik. 2008. Amyloid fibrillar meshwork formation of iron-induced oligomeric species of Aβ40 with phthalocyanine tetrasulfonate and its toxic consequences. *ChemBioChem.* 9:2602–2605.

42. Tabassum, S., A. M. Sheikh, …, A. Nagai. 2015. A carboxylated Zn-phthalocyanine inhibits fibril formation of Alzheimer's amyloid β peptide. *FEBS J.* 282:463–476.

43. Fezoui, Y., D. M. Hartley, …, D. B. Teplow. 2000. An improved method of preparing the amyloid β-protein for fibrillogenesis and neurotoxicity experiments. *Amyloid.* 7:166–178.

44. Valiente-Gabioud, A. A., M. C. Miotto, …, C. O. Fernández. 2016. Phthalocyanines as molecular scaffolds to block disease-associated protein aggregation. *Acc. Chem. Res.* 49:801–808.

45. Binolfi, A., E. E. Rodriguez, …, C. O. Fernández. 2010. Bioinorganic chemistry of Parkinson's disease: structural determinants for the copper-mediated amyloid formation of α-synuclein. *Inorg. Chem.* 49:10668–10679.

46. Bouter, Y., K. Dietrich, …, T. A. Bayer. 2013. N-truncated amyloid β (Aβ) 4-42 forms stable aggregates and induces acute and long-lasting behavioral deficits. *Acta Neuropathol.* 126:189–205.

47. Scopes, R. K., and J. A. Smith. 2001. Analysis of Proteins. *In* Current Protocols in Molecular Biology. John Wiley & Sons, Hoboken, NJ.

48. Chevallet, M., S. Luche, and T. Rabilloud. 2006. Silver staining of proteins in polyacrylamide gels. *Nat. Protoc.* 1:1852–1858.

49. Cavanagh, J. 2007. Protein NMR Spectroscopy Principles and Practice. Academic Press, Amsterdam, the Netherlands.

50. Rezaei-Ghaleh, N., S. Kumar, …, M. Zweckstetter. 2016. Phosphorylation interferes with maturation of amyloid-β fibrillar structure in the N terminus. *J. Biol. Chem.* 291:16059–16067.

51. Feng, B. Y., B. H. Toyama, …, B. K. Shoichet. 2008. Small-molecule aggregates inhibit amyloid polymerization. *Nat. Chem. Biol.* 4:197–199.

52. Hill, J. S., S. B. Kahl, …, A. H. Kaye. 1995. Selective tumor kill of cerebral glioma by photodynamic therapy using a boronated porphyrin photosensitizer. *Proc. Natl. Acad. Sci. USA.* 92:12126–12130.

53. Stylli, S., J. Hill, …, A. Kaye. 1995. Aluminium phthalocyanine mediated photodynamic therapy in experimental malignant glioma. *J. Clin. Neurosci.* 2:146–151.

54. Dee, D. R., A. N. Gupta, …, M. T. Woodside. 2012. Phthalocyanine tetrasulfonates bind to multiple sites on natively-folded prion protein. *Biochim. Biophys. Acta.* 1824:826–832.

55. Alies, B., I. Sasaki, …, C. Hureau. 2013. Zn impacts Cu coordination to amyloid-β, the Alzheimer's peptide, but not the ROS production and the associated cell toxicity. *Chem. Commun. (Camb.).* 49:1214–1216.

56. Faller, P., and C. Hureau. 2009. Bioinorganic chemistry of copper and zinc ions coordinated to amyloid-β peptide. *Dalton Trans.* 38:1080–1094.

57. Petkova, A. T., Y. Ishii, …, R. Tycko. 2002. A structural model for Alzheimer's β-amyloid fibrils based on experimental constraints from solid state NMR. *Proc. Natl. Acad. Sci. USA.* 99:16742–16747.

58. Petkova, A. T., W. M. Yau, and R. Tycko. 2006. Experimental constraints on quaternary structure in Alzheimer's β-amyloid fibrils. *Biochemistry.* 45:498–512.

59. Yu, L., R. Edalji, …, E. T. Olejniczak. 2009. Structural characterization of a soluble amyloid β-peptide oligomer. *Biochemistry.* 48:1870–1877.

60. Palewska, K., J. Sworakowski, and J. Lipiński. 2012. Molecular aggregation in soluble phthalocyanines—Chemical interactions vs. π-stacking. *Opt. Mater.* 34:1717–1724.

61. Danielsson, J., J. Jarvet, …, A. Gräslund. 2005. The Alzheimer beta-peptide shows temperature-dependent transitions between left-handed 3-helix, β-strand and random coil secondary structures. *FEBS J.* 272:3938–3949.

62. Danielsson, J., R. Pierattelli, …, A. Gräslund. 2007. High-resolution NMR studies of the zinc-binding site of the Alzheimer's amyloid β-peptide. *FEBS J.* 274:46–59.

63. Alies, B., V. Pradines, …, P. Faller. 2011. Zinc(II) modulates specifically amyloid formation and structure in model peptides. *J. Biol. Inorg. Chem.* 16:333–340.

64. Alies, B., P. L. Solari, …, P. Faller. 2012. Dynamics of Zn(II) binding as a key feature in the formation of amyloid fibrils by Aβ11–28. *Inorg. Chem.* 51:701–708.

65. Yuan, C., and Z. Gao. 2013. Aβ interacts with both the iron center and the porphyrin ring of heme: mechanism of heme's action on Aβ aggregation and disaggregation. *Chem. Res. Toxicol.* 26:262–269.

66. Ghosh, C., S. Mukherjee, …, S. G. Dey. 2016. Peroxidase to cytochrome b type transition in the active site of heme-bound amyloid β peptides relevant to Alzheimer's disease. *Inorg. Chem.* 55:1748–1757.

Biophysical Journal, Volume *114*

Supplemental Information

Binding Modes of Phthalocyanines to Amyloid β Peptide and Their Effects on Amyloid Fibril Formation

Ariel A. Valiente-Gabioud, Dietmar Riedel, Tiago F. Outeiro, Mauricio A. Menacho-Márquez, Christian Griesinger, and Claudio O. Fernández

Supplementary Figure 1

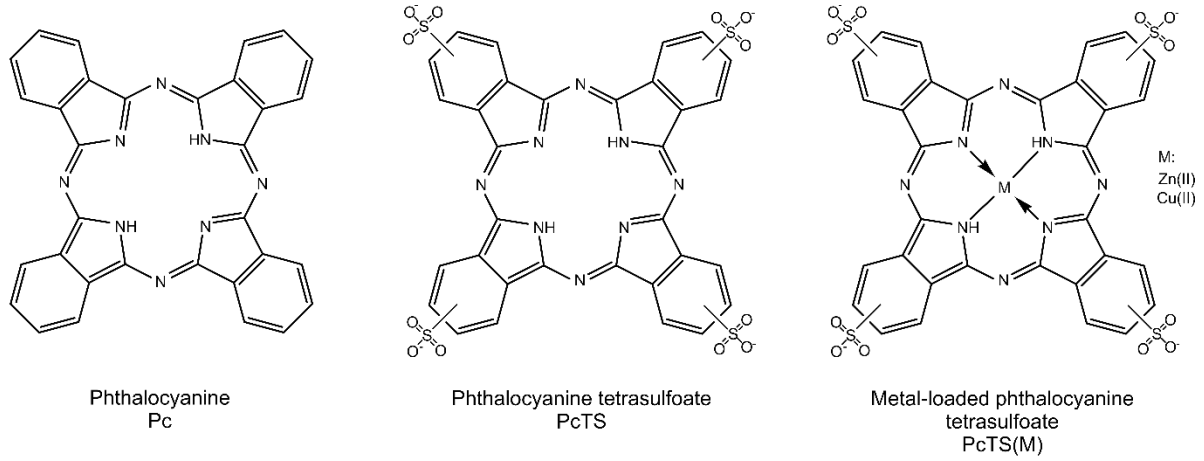

Figure S1: Schematic representation of Phthalocyanine structure. The basic backbone is presented (Pc), as well as the tetrasulfonate form (PcTS) and the metal derivatives studied in this work (PcTS(M)).

Supplementary Figure 2

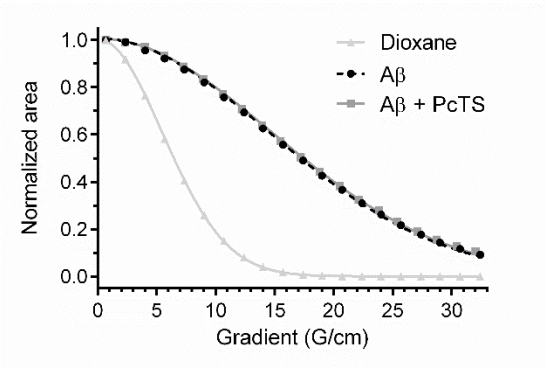

Figure S2: NMR signal decay observed for the free (black circles) and PcTS-complexed (dark grey squares) states of $A\beta_{40}$ at 15 °C in pulsed field gradient NMR experiments. To estimate the hydrodynamic radius, the signal decay of dioxane was also recorded (light grey triangles). The data shows that free and PcTS-bound $A\beta_{40}$ have identical diffusion coefficients, in agreement with a similar assembly state.

Supplementary Figure 3

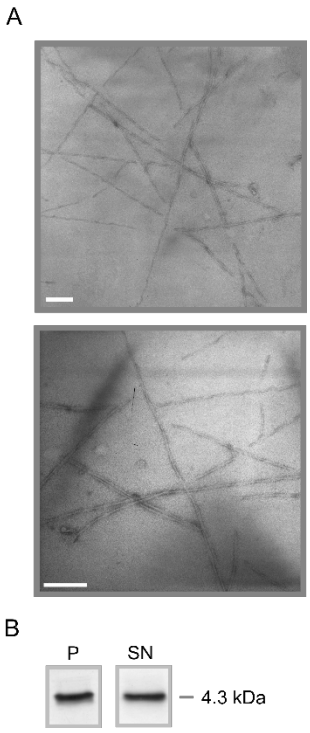

Figure S3: Analysis of PcTS[Cu(II)] effects on $A\beta_{40}$ amyloid assembly. (A) Representative negative-stain EM images of $A\beta_{40}$ aggregates (50 μM $A\beta_{40}$ samples) generated in the presence of 150 μM PcTS(Cu(II)) (Scale bars, 100 nm). (B) SDS/PAGE analysis of $A\beta_{40}$ peptide soluble (SN) and insoluble (P) fractions of the end point of the aggregation assays in the presence of 3 equivalents of PcTS(Cu(II)).

Supplementary Figure 4

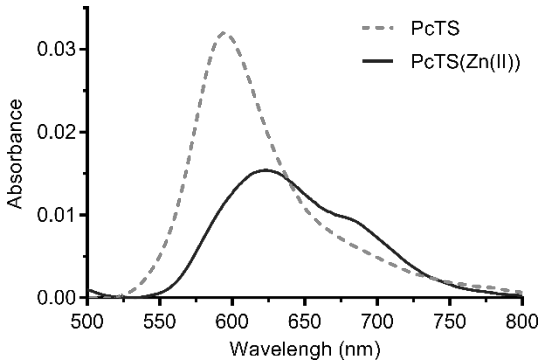

Figure S4: Electronic absorption spectra corresponding to the pellet fraction of 50 μM $A\beta_{40}$ aggregations obtained in the presence of 150 μM PcTS(Zn(II)) (continuous line) or PcTS (dashed line).